

# Targeting Root Cause by Systemic scAAV9-h/IDS Gene Delivery: Functional Correction and Reversal of Severe MPS II in Mice

Haiyan Fu,<sup>1,4</sup> Kim Zaraspe,<sup>1,5</sup> Naoko Murakami,<sup>1,5</sup> Aaron S. Meadows,<sup>1</sup> Ricardo J. Pineda,<sup>1</sup> Douglas M. McCarty,<sup>1,2,5</sup> and Joseph Muenzer<sup>3</sup>

<sup>1</sup>Center for Gene Therapy, Research Institute at Nationwide Children's Hospital, Columbus, OH 43205, USA; <sup>2</sup>Department of Pediatrics, School of Medicine, The Ohio State University, Columbus, OH, USA; <sup>3</sup>Division of Genetics and Metabolism, Department of Pediatrics, School of Medicine, University of North Carolina at Chapel Hill, Chapel Hill, NC 27514, USA

**No treatment is available to address the neurological need and reversibility of MPS II. We developed a scAAV9-hIDS vector to deliver the human iduronate-2-sulfatase gene and test it in mouse model. We treated MPS II mice at different disease stages with an intravenous injection of scAAV9-mCMV-hIDS at different doses. The treatments led to rapid and persistent restoration of IDS activity and the reduction of glycosaminoglycans (GAG) throughout the CNS and somatic tissues in all cohorts. Importantly, the vector treatment at up to age 6 months improved behavior performance in the Morris water maze and normalized the survival. Notably, vector treatment at age 9 months also resulted in persistent rIDS expression and GAG clearance in MPS II mice, and the majority of these animals survived within the normal range of lifespan. Notably, the vector delivery did not result in any observable adverse events or detectable systemic toxicity in any treated animal groups. We believe that we have developed a safe and effective gene therapy for treating MPS II, which led to recent IND approval for a phase 1/2 clinical trial in MPS II patients, further supporting the extended potential of the demonstrated systemic rAAV9 gene delivery platform for broad disease targets.**

## INTRODUCTION

Mucopolysaccharidosis (MPS) II, or Hunter syndrome, is a rare X-linked genetic disorder, predominately a disease of males.<sup>1</sup> The disease is caused by the gene defects in iduronate-2-sulfatase (IDS), a lysosomal enzyme essential for the stepwise degradation of biologically important glycosaminoglycans (GAGs), heparan sulfates (HSs), and dermatan sulfates (DSs). While the mutations are highly heterogeneous, the lack of or reduced IDS activity results in the accumulation of undegraded or partially degraded HS and DS GAGs in cells in virtually all organs, leading to progressive multisystem disorders. Patients with MPS II typically appear normal at birth, with the symptoms becoming apparent between 2 and 4 years of age. While the severity of the disease varies widely among individuals, clinically, there are 2 forms of MPS II: attenuated and severe. While both forms develop broad peripheral organ manifestations, the majority (2/3) of MPS II patients have the severe form of the disease, with more severe

somatic involvement and prominent neurological disorders that manifest as developmental delays, progressive neurodegeneration, and cognitive impairment beginning by the age of 2 years. In the severe form, death generally occurs by 10–15 years of age from neurological, cardiac, or pulmonary disorders, though some with attenuated MPS II can live to adulthood.

The current standard of care for MPS II is recombinant enzyme replacement therapy (ERT) (Elaprase) delivered intravenously (i.v.), with demonstrated improvements in somatic symptoms in both severe and attenuated patients.<sup>2</sup> Systemic ERT must be administered weekly for life. Notably, ERT delivered i.v. does not cross the blood-brain barrier (BBB) and, therefore, does not treat neurological disorders. Intrathecal (IT) ERT has been developed to target the CNS by delivering recombinant IDS (rIDS) into the cerebrospinal fluid (CSF).<sup>3</sup> However, based on the recent results from the phase 2/3 IT ERT clinical trial of SHP609 (Shire) (ClinicalTrials.gov: NCT02055118), the study did not meet either its primary or its key secondary endpoint, but the trial is ongoing. Furthermore, this IT ERT would remain costly and invasive and would require routine repetitive enzyme infusion to maintain therapeutic effects. Hematopoietic stem cell transplantation (HSCT) has been used as a treatment for attenuated MPS II with some benefit but is not recommended for MPS II patients with neurological impairment. No treatment is

Received 11 May 2018; accepted 10 July 2018;  
<https://doi.org/10.1016/j.omtm.2018.07.005>

<sup>4</sup>Present address: Department of Pediatrics, School of Medicine, University of North Carolina at Chapel Hill, Chapel Hill, NC 27514, USA.

<sup>5</sup>Present address: Pfizer/Bamboo Therapeutics, 7030 Kit Creek Rd., Morrisville, NC 27560, USA.

**Correspondence:** Haiyan Fu, PhD, Department of Pediatrics, School of Medicine, University of North Carolina at Chapel Hill, Chapel Hill, NC 27599, USA.

**E-mail:** [hfu@email.unc.edu](mailto:hfu@email.unc.edu)

**Correspondence:** Joseph Muenzer, PhD, Division of Genetics and Metabolism, Department of Pediatrics, School of Medicine, University of North Carolina at Chapel Hill, Chapel Hill, NC 27599, USA.

**E-mail:** [muenzer@med.unc.edu](mailto:muenzer@med.unc.edu)



currently available to treat the CNS disorders in the severe form of MPS II.

Gene therapy promises an ideal treatment for the majority of lysosomal storage diseases (LSDs), because it targets the root cause by replacing the defective gene and has the potential for long-term endogenous production of recombinant enzymes without the need to transduce every cell, given the bystander effects of lysosomal enzymes. Numerous viral-vector-mediated gene therapy studies, mostly designed to restore missing enzyme activity, have shown various degrees of correction of lysosomal storage *in vitro* and *in vivo* in LSD animal models, using retroviral, adenoviral, herpes, and recombinant adeno-associated virus (rAAV) vectors.<sup>4</sup> rAAV is an ideal vector for this application because of long-term transduction and its safe profiles, with different AAV serotypes displaying diverse tissue tropisms.<sup>5–8</sup>

While AAV was shown to mediate long-term transduction and correction of lysosomal storage pathology in the brain and somatic tissues in mouse models,<sup>9–15</sup> the mode of delivery remains the key to achieve widespread CNS transduction. To date, numerous CNS gene therapy studies for MPS disorders have been performed using direct brain parenchymal injection, with localized transduction and partial correction of lysosomal storage in MPS I, IIIB, and VII mice.<sup>11–15</sup> Given the global neuropathies in LSDs, direct brain injection may not be feasible for treating MPS disorders in humans, though rAAV gene therapy clinical trials for Batten disease, Canavan disease, metachromatic leukodystrophy, and MPS IIIA showed that direct brain AAV vector injections were safe.<sup>9,16,17</sup> More efforts have also been made to develop approaches for more efficient AAV CNS gene delivery and functional benefits for treating neuropathic LSDs.<sup>18–20</sup>

The more recent demonstration of rAAV9 trans-BBB neurotropism has offered an effective solution for CNS gene delivery,<sup>21,22</sup> leading to successes in developing approaches for the treatment of neurological diseases, including MPS II, in animal models via systemic<sup>23–30</sup> or IT delivery.<sup>27,31–38</sup> These studies have led to ongoing clinical trials of systemic rAAV9 gene delivery in patients with spinal muscular atrophy (SMA) (ClinicalTrials.gov: NCT02122952), MPS IIIA (ClinicalTrials.gov: NCT02716246), and MPS IIIB (ClinicalTrials.gov: NCT03315182), and IT gene delivery for giant axonal neuropathy (NCT02362438), MPS I (RGX-111, RegenxBio), and MPS II (RGX121, RegenxBio). Furthermore, gene therapy studies using liver-targeting, AAV-mediated zinc-finger nuclease (ZFN) gene-editing approaches<sup>39</sup> have advanced to clinical trials for MPS I (ClinicalTrials.gov: NCT02702115) and MPS II (ClinicalTrials.gov: NCT03041324) using AAV6 via delivery *i.v.*, which were designed to treat somatic manifestations of these diseases. In addition, liver gene transfer using AAV8 in a feline model<sup>40</sup> led to a phase 1/2 gene therapy clinical trial for MPS VI (ClinicalTrials.gov: NCT03173521). Notably, all these AAV products target the root cause, the gene defects of the specific lysosomal enzymes.

In this study, we developed a self-complementary (sc)AAV9-hIDS vector that targets the root cause of MPS II and demonstrated great therapeutic potential and safe profiles for treating MPS II in mice via a single injection *i.v.* Notably, this study has led to the recent investigational new drug (IND) approval by the US Food and Drug Administration (FDA) for a phase 1/2 gene therapy clinical trial in patients with MPS II (IND# 17838).

## RESULTS

To assess the therapeutic potential of systemic scAAV9-mCMV-hIDS gene delivery, we treated 1-month-old MPS II mice with an *i.v.* injection of scAAV9-mCMV-hIDS vector at  $2.5 \times 10^{12}$  vg/kg or  $5 \times 10^{12}$  vg/kg ( $n = 20$  per group). To expand the clinical relevance and assess the reversibility of MPS II pathology, we also treated mice at age 3 months, 6 months, or 9 months with an *i.v.* injection of scAAV9-mCMV-hIDS at different doses ( $n = 18–20$  per group). The animals were tested for behavior performance in a hidden task in a Morris water maze at age 8 months and/or 12 months ( $n = 13–16$  per group). Necropsies were performed for tissue analyses at 1 month post-injection (pi), age 8 months, or humane endpoint ( $n = 4–6$  per group). Subsets of animals in each cohort were observed for longevity. Randomly assigned non-treated MPS II mice and their male wild-type (WT) littermates are used as controls. Table 1 summarizes the overall experimental design.

### Persistent Global Restoration of Functional IDS in the CNS, PNS, and Somatic Tissues

To assess the levels and persistence of transgene expression, tissues were assayed for IDS activity at 1 month pi, age 8 months, or humane endpoint (Table 1). An *i.v.* injection of  $5 \times 10^{12}$  vg/kg scAAV9-mCMV-hIDS vector resulted in rapid and persistent restoration of IDS activity to supranormal levels in the liver, heart, lung, skeletal muscle, spleen, and intestine and to 14% of WT levels in the brain (Figure 1A), though there was a decrease over time between 1 month pi, age 8 months, and endpoint. Similarly, we detected IDS activity at supranormal levels in the majority of the tested tissues and 6% of WT levels in the brain in MPS II mice treated at age 1 month with  $2.5 \times 10^{12}$  vg/kg scAAV9-mCMV-hIDS (Figure 1B). Further, we also detected effective restoration of tissue IDS activity in MPS II mice treated at age 3 months, 6 months, or 9 months with an *i.v.* injection of the vector at  $5 \times 10^{12}$  vg/kg,  $1 \times 10^{13}$  vg/kg, or  $2 \times 10^{13}$  vg/kg (Figures 1C–E). Importantly, the AAV-mediated IDS activity persisted to the endpoints in all tissues (Figure 1). Notably, there was no detectable IDS activity in tissues in non-treated MPS II mice.

### Long-Term Clearance of Lysosomal Storage Pathology and Astrocytosis

To assess the therapeutic impact of systemic scAAV9-hIDS gene delivery in MPS II mice, tissues were assayed for GAG contents, at 1 month pi, age 8 months, or humane endpoint. Our results showed a significant reduction of GAG contents to WT levels in all tested tissues, including brain, with the exception of spleen, in MPS II

**Table 1. Study Design: Systemic scAAV9-mCMV-hIDS Gene Delivery in MPS II Mice**

Mice	Vector Dose (vg/kg)	Injection Age (Months)	No. of Animals						
			Total	Behavior Testing	Necropsy				Longevity
					1 Month pi	Age 8 Months	Age 12 Months	Endpoint	
MPS II	$2.5 \times 10^{12}$	1	20	15 <sup>a</sup>	5	5	0	6	10
MPS II	$5 \times 10^{12}$	1	20	15 <sup>a</sup>	5	5	0	5	10
MPS II	$5 \times 10^{12}$	3	19	13 <sup>a</sup>	5	5	0	5	9
MPS II	$5 \times 10^{12}$	6	19	14 <sup>b</sup>	4	4	0	6	11
MPS II	$1 \times 10^{13}$	6	22	16 <sup>b</sup>	4	5	0	4	13
MPS II	$2 \times 10^{13}$	6	18	14 <sup>c</sup>	4	5	0	4	9
MPS II	$2 \times 10^{13}$	9	19	0	4	0	4	4	11
WT	0	N/A	86 <sup>d</sup>	83 <sup>d</sup>	2	10	0	–	74 <sup>d</sup>
MPS II	0	N/A	24	20	1	5	0	3	18

<sup>a</sup>Tested at age 8 months.  
<sup>b</sup>Tested at age 8 months and re-tested at age 12 months.  
<sup>c</sup>Tested at age 12 months.  
<sup>d</sup>Combined data from multiple studies.

mice treated at age 1 month, 3 months, 6 months, or 9 months with an i.v. injection of scAAV9-mCMV-hIDS at doses of  $2.5 \times 10^{12}$  vg/kg (Figure 2A),  $5 \times 10^{12}$  vg/kg (Figures 2B–2D),  $1 \times 10^{13}$  vg/kg (Figure 2E), or  $2 \times 10^{13}$  vg/kg (Figures 2F and 2G). These data indicate that the scAAV9-mediated rIDS is functional and sufficient for the complete clearance of GAG storage in the CNS and periphery, even when treating MPS II mice at advanced disease stages (Figures 2D–2G). Furthermore, these data correlate to the tissue IDS activity levels (Figure 1) and the functional benefits (Figure 5).

To further assess the effects of the vector treatment on the lysosomal storage pathology, brain and peripheral tissues were also assayed by immunofluorescence (IF) for lysosomal-associated membrane protein 1 (LAMP1) at 1 month pi, age 8 months, or endpoint. The results showed the clearance of excessive LAMP1 throughout the brain (Figure 3A), in intestinal neurons (Figure 3B), and in retina (Figure 3C) in the vector-treated MPS II mice at all tested time points, indicating the efficient long-term correction and reversal of lysosomal storage pathology in the CNS, peripheral nervous system (PNS), optical nervous system (ONS), and periphery. In addition, significant reduction in LAMP1 staining was also observed in non-neuronal tissues of the eye, including cornea, ciliary process, and iris (Figure 4A), as well as in broad somatic tissues (Figure 4B), indicating correction of lysosomal storage in the periphery. However, the vector treatment led to partial reduction of LAMP1 in the kidney (Figure 4B).

Further, IF staining also showed a significant decrease in glial fibrillary acidic protein (GFAP)-positive cells/signals in gray matter throughout the brain (Figure 3A), in the submucosal plexus and myoenteric plexus in intestine (Figure 3B), and in retina (Figure 3C),

demonstrating the correction of astrocytosis and neuroinflammation in the CNS, PNS, and ONS.

#### Significant Improvement in Behavioral Performance

To assess the functional impact of a systemic scAAV9-hIDS gene delivery, vector-treated mice and controls ( $n \geq 13$  per group) were tested for cognitive ability and motor function in a hidden task in the Morris water maze, when they were 8 months old. The results showed normalized latency to find a hidden platform and swimming ability in MPS II mice that received an i.v. injection of  $2.5 \times 10^{12}$  vg/kg or  $5 \times 10^{12}$  vg/kg scAAV9-mCMV-hIDS at age 1 month or 3 months (Figures 5A and 5B), indicating the correction of cognitive and motor functions. We also observed normalized swimming ability and improved, though not normalized, latency to the find the hidden platform in MPS II mice that were treated at age 6 months with  $5 \times 10^{12}$  vg/kg or  $1 \times 10^{13}$  vg/kg vector when tested at age 8 months, only 2 months pi (Figures 5B–5D). Notably, further improvements in behavior performance in the water maze were observed when these mice were re-tested at age 12 months (Figures 5C and 5D), because the full scale of functional benefits may require more time when treated at very advanced disease stages. MPS II mice treated with  $2 \times 10^{13}$  vg/kg vector were only tested at age 12 months and showed partial improvement, compared to 8-month-old non-treated MPS II mice. Notably, the majority of non-treated MPS II mice >8 months of age are not testable in a water maze due to disease severity. These data demonstrate that a single i.v. injection of scAAV9-mCMV-hIDS at an effective dose can not only prevent but may also reverse the cognitive and motor functions to a certain extent in MPS II mice.

#### Extension in Survival

A subset of each cohort was observed for longevity (Figure 5F) to further assess the functional benefits of the vector treatments. The

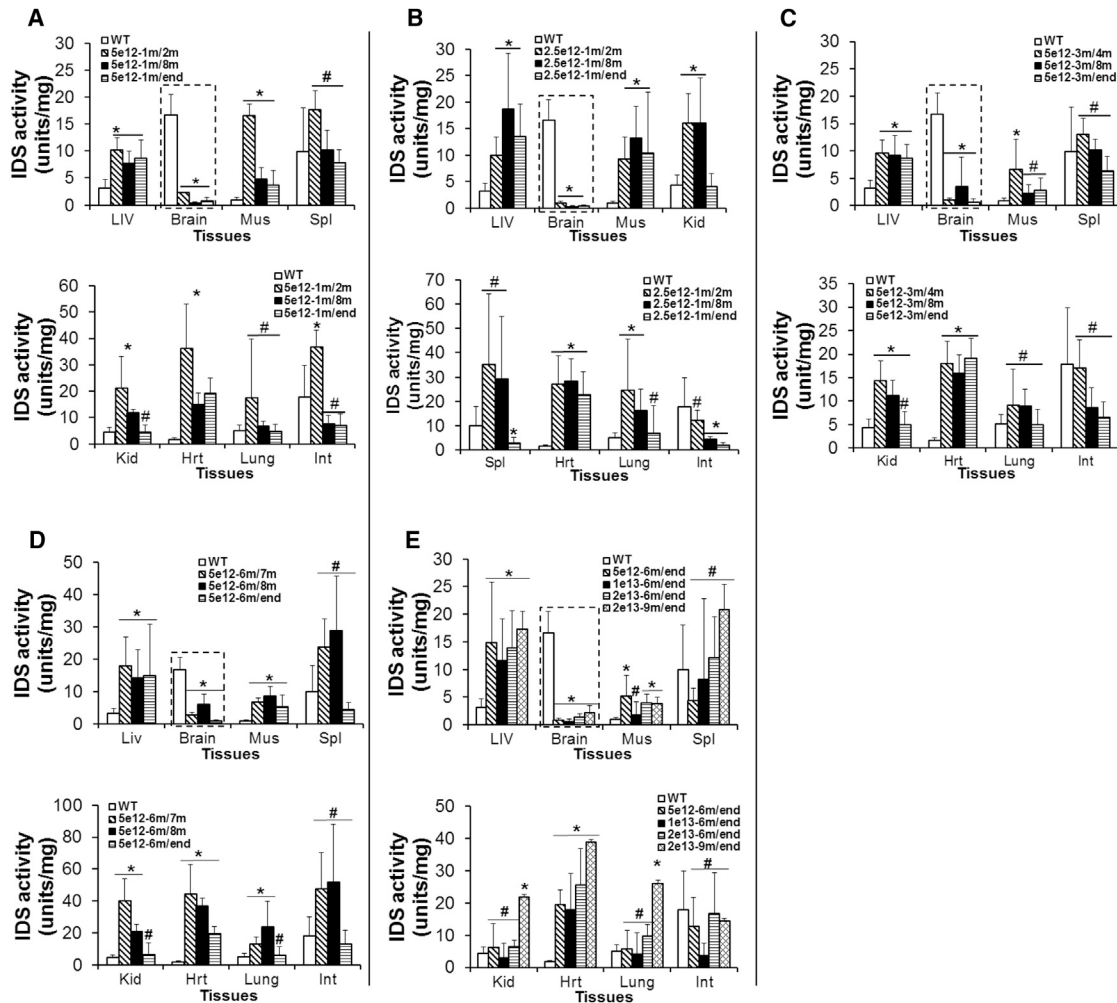


**Figure 1. Persistent rIDS Expression in the CNS and Peripheral Tissues after a Systemic scAAV9.hIDS Gene Delivery**

(A–E) MPS II mice were treated at age 1 month (A and B), 3 months (C), 6 months (D and E), or 9 months (E) with an i.v. injection of scAAV9-mCMV.hIDS at  $5 \times 10^{12}$  vg/kg (A and C–E),  $2.5 \times 10^{12}$  vg/kg (B),  $1 \times 10^{13}$  vg/kg (E), or  $2 \times 10^{13}$  vg/kg (E). Tissues were assayed for IDS activity at 1 month pi, 8 months of age, or humane endpoint. IDS activity is expressed as units per milligram of protein; 1 U = 1 nmol 4MU released per hour. WT, non-treated WT mice; m/m, injection age/testing age; Liv, liver; Mus, skeletal muscle; Spl, spleen; Kid, kidney; Hrt, heart; Int, intestine. \* $p < 0.05$  versus WT; # $p > 0.05$  versus WT (t test).  $n = 4$ –6 per group.

mice were observed for humane endpoint criteria, including urine retention, rectal prolapse, penile prolapse, and immobility. The vector treatments resulted in significant extension of survival in all treatment cohorts, compared to non-treated MPS II mice ( $p < 0.05$ ; Figure 5F). The survival of MPS II mice treated with  $5 \times 10^{12}$  vg/kg scAAV9-mCMV-hIDS was similar to that of WT controls, with no detectable difference in longevity between mice treated at ages 1 month, 3 months, and 6 months (Figure 5F). The majority of MPS II mice treated at age 1 month with  $2.5 \times 10^{12}$  vg/kg vector also lived within the range of the WT lifespan (Figure 5F). More importantly, most of the MPS II mice treated at age 6 months or 9 months with higher vector doses ( $1 \times 10^{13}$  vg/kg or  $2 \times 10^{13}$  vg/kg) also survived within the normal range of lifespan (Figure 5F). Given that neurological manifestation is one of the major causes of premature death in MPS II, the significantly extended

survival further supports the functional therapeutic benefits of systemic scAAV9-mCMV-hIDS gene delivery for treating MPS II.

#### Differential Biodistribution of rAAV9-mCMV-hIDS Vector Genome

To determine the biodistribution of the systemically delivered scAAV9-mCMV-hIDS, total DNA isolated from tissues was assayed by qPCR to quantify scAAV9-hIDS vector genome (vg) copy numbers in tissues at different time points post-vector injection ( $n \geq 4$  per group). The results showed differential biodistribution of the vector DNA among different tissues, with the highest concentration detected in the liver, followed by heart, skeletal muscle, lung, intestine, kidney, spleen, and brain (Figure 6). The vg copies in tissues persisted, though decreases of vg were observed in some tissues over time between ages 2 months and

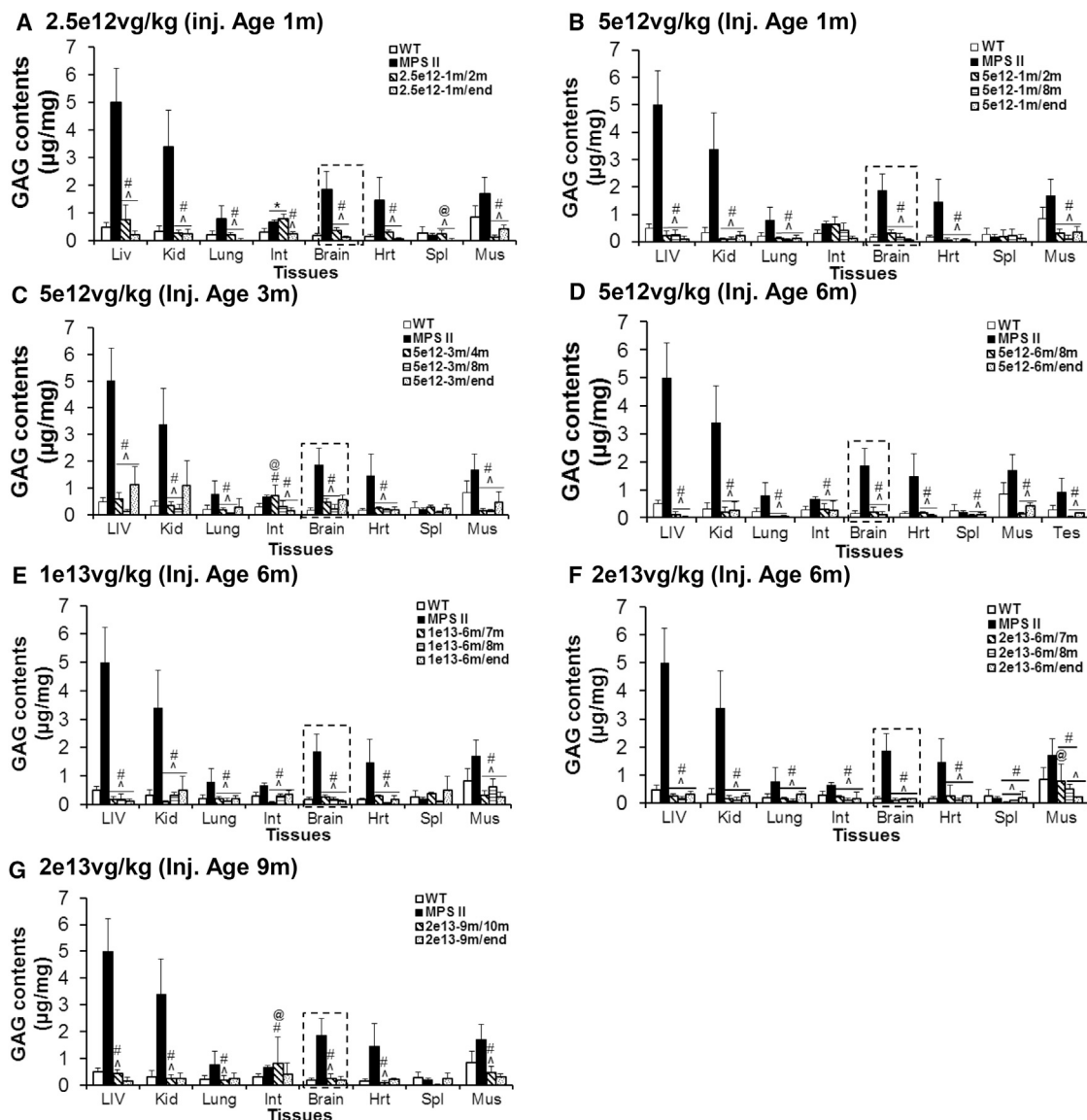


**Figure 2. Significant Reduction of GAG Content in the CNS and Peripheral Tissues in MPS II Mice following a Systemic scAAV9-hIDS Gene Delivery**  
 MPS II mice were treated at age 1 month (A and B), 3 months (C), 6 months (D–F), or 9 months (G) with an i.v. injection of scAAV9-mCMV-hIDS at  $2.5 \times 10^{12}$  vg/kg (A),  $5 \times 10^{12}$  vg/kg (B–D),  $1 \times 10^{13}$  vg/kg (E), or  $2 \times 10^{13}$  vg/kg (F and G). Tissues were assayed for GAG contents at 1 month pi, age 8 months, or humane endpoint ( $n \geq 4$  per group). GAG content is expressed as micrograms per milligram of wet tissue. WT, non-treated WT mice; MPS II, non-treated MPS II mice; m/m, injection age/testing age in months; LIV, liver; Kid, kidney; Int, intestine; Hrt, heart; Spl, spleen; Mus, skeletal muscle. \* $p \leq 0.05$  versus WT; # $p > 0.05$  versus WT; ^ $p \leq 0.05$  versus non-treated MPS II; @ $p > 0.05$  versus non-treated MPS II (t test).

8 months. Our data also showed the dose responses in the bio-distribution of the vg. Similar differential biodistribution profiles were also observed in MPS II and WT mice receiving high doses of vector in our bridge toxicology (Figure S2).

**Histopathology Analysis: No Vector Treatment-Associated Systemic Toxicity**

To assess potential toxicity, tissue sections from MPS II mice treated with scAAV9-mCMV-hIDS and their WT and non-treated

MPS II littermates were processed for H&E staining at 1 month pi, age 8 months, or humane endpoint and then examined for histopathology by a licensed veterinary pathologist at GEMpath (Longmont, CO, USA). The examined tissues include brain and multiple somatic tissues (liver, kidney, spleen, heart, lung, intestine, and skeletal muscle). Histopathology examination was also performed to analyze tissues from MPS II and WT mice treated with the vector at a high dose ( $5 \times 10^{13}$  vg/kg) in the bridge toxicology testing.



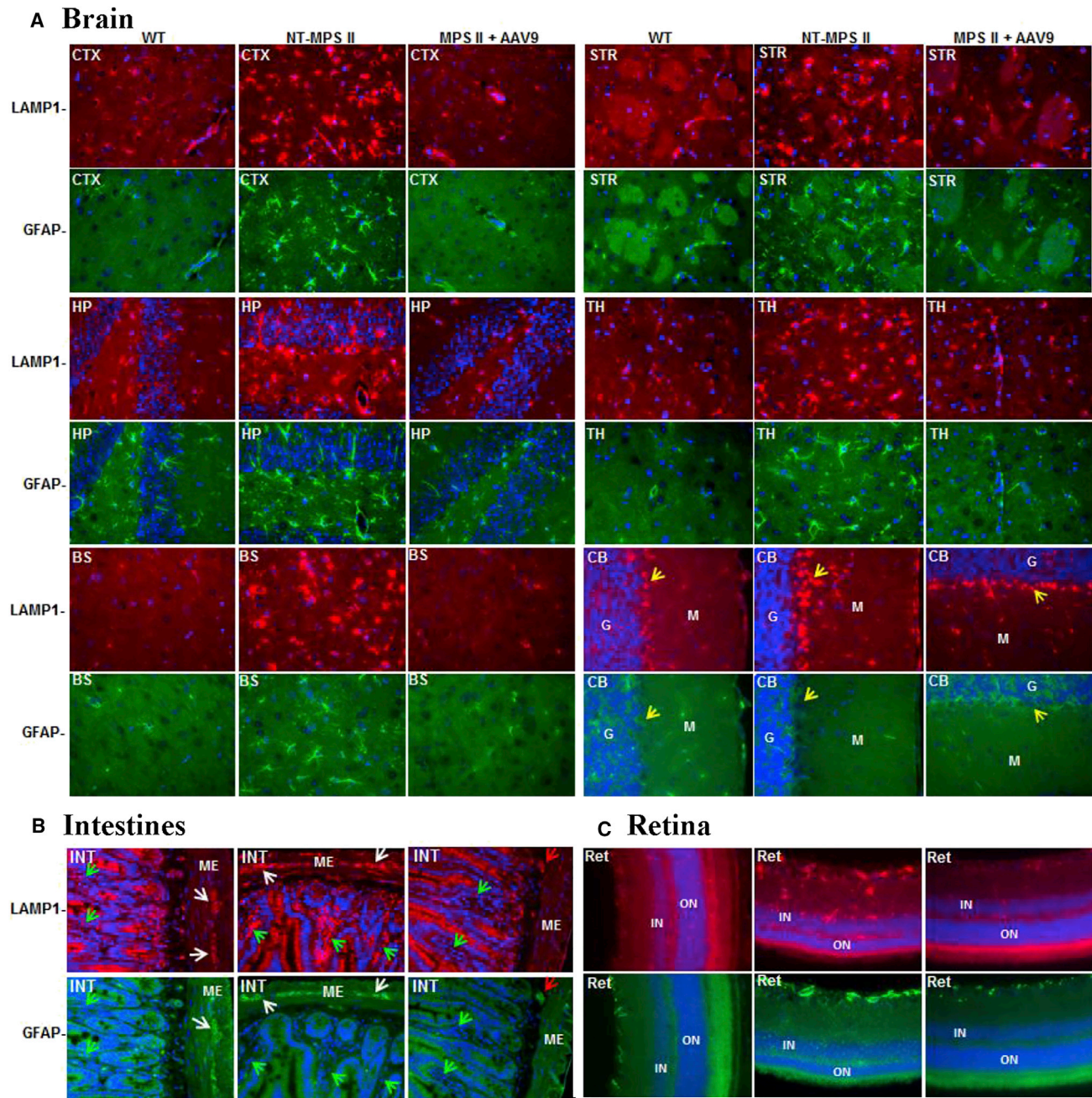


**Figure 3. Correction of Lysosomal Storage and Astrocytosis in the CNS, PNS, and ONS in MPS II Mice following a Systemic scAAV9-hIDS Gene Delivery**  
MPS II mice were treated with an i.v. injection of  $5 \times 10^{12}$  vg/kg scAAV9-mCMV-hIDS at age 1 month. Tissues were assayed at age 8 months (7 months pi) by immunofluorescence for LAMP 1 (red fluorescence) and GFAP (green fluorescence). WT, WT controls; NT-MPS II, non-treated MPS II controls; MPS II+AAV9, vector-treated MPS II mouse. (A) Brain. CTX, cerebral cortex; STR, striatum; HP, hippocampus; TH, thalamus; BS, brain stem; CB, cerebellum. G, granule layer; M, molecular layer. Yellow arrows indicate Purkinje cell layer. (B) Intestine. INT, small intestine; ME, muscularis externa. White arrows indicate neurons of myenteric plexus; red arrows indicate neurons of submucosa plexus; green arrows indicate lamina propria. (C) Retina of eye. RET, retina; ON, outer nuclear layer; IN, inner nuclear layer.

The pathology examination showed no vector treatment-associated systemic toxicity in MPS II and/or WT mice treated with an i.v. injection of scAAV9-mCMV-hIDS at doses of  $2.5 \times$

$10^{12}$  vg/kg to  $5 \times 10^{13}$  vg/kg. These data strongly support the safe profiles of systemic scAAV9-mCMV-hIDS gene delivery for treating MPS II.

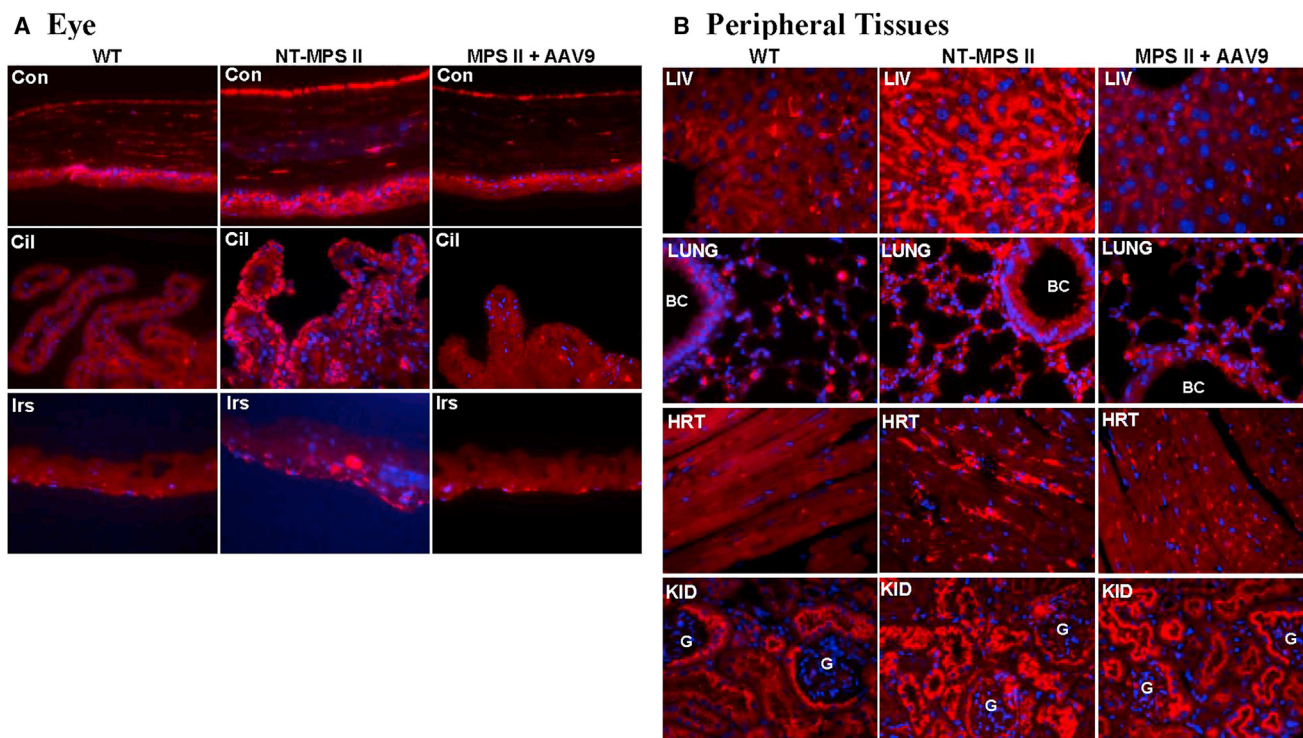


**Figure 4. AAV-Mediated Correction of Lysosomal Storage in Non-neuronal Tissues in Eyes and Peripheral Tissues**

(A and B) MPS II mice were injected i.v. with  $5 \times 10^{12}$  vg/kg scAAV9-mCMV-hIDS at age 1 month. Eye (A) and peripheral tissues (B) were assayed at 7 months pi (age 8 months) by immunofluorescence for LAMP 1 (red fluorescence). Blue fluorescence indicates DAPI-stained nuclei. Con, cornea; Cil, ciliary process; Irs, iris; LIV, liver; BC, bronchiole; HRT, heart; KID, kidney. G, glomerulus.

#### Tumor Occurrence at a Rate Similar to that in WT Mice

As described earlier, longevity studies were performed in a subset of animals (Table 1), and necropsies were performed and tissues were analyzed at humane endpoints. Among necropsied mice (Table 2), tumors were observed in the liver by gross examination and/or by histopathology analyses, in 15 of 42 (35.7%) vector-treated MPS II mice (ages 16–25 months) and 9 of 25 (36.0%) non-treated WT mice (ages 23–29 months), indicating very similar tumor incidences between the vector-treated MPS II and WT mice ( $p = 0.9833$ ). The majority of tumors were identified by gross examination, and histopathology examination identified microscopic tumors in non-tumor tissues in 2 vector-treated MPS II mice (Table S1), while no microscopic tumors were observed in the non-tumor tissues in the majority of vector-treated mice. Our data showed that tumor incidence in MPS II mice was not dose dependent ( $p > 0.55$ ), with higher tumor incidence in mice treated at age 1 month than in mice treated at age 6 months, though statistically insignificant ( $p = 0.314$ ).

To determine the potential genotoxicity, qPCR was performed to analyze total DNA samples from tumors and detected the vg in all tested tumors ( $0.021\text{--}38.5 \times 10^5$  vg/ $\mu$ g genomic DNA [gDNA]) from 13 AAV9-treated mice (Table S1). No detectable vg was observed in tumors from non-treated WT mice ( $<0.001 \times 10^5$  vg/ $\mu$ g gDNA).

#### DISCUSSION

We demonstrate here the rapid and persistent therapeutic effects of a systemic scAAV9-mCMV-hIDS gene delivery for the treatment of MPS II. Within as early as 5 days of the treatment, an i.v. injection of the vector led to the effective restoration of IDS enzyme activity. The functional rIDS persisted over the lifetime, leading to the clearance of stored GAG throughout the CNS and in broad somatic tissues in MPS II mice. This rapid and persistent effect supports the potential of this approach for treating MPS II patients, which may halt disease progression and have permanent therapeutic effects.

The majority of the patients with MPS II are diagnosed after age 1–2 years, when observable neurological and somatic disorders have already taken place. Therefore, the reversibility of the disease, especially the severe form, has been a major concern in therapeutic development. In this study, we demonstrated that an i.v. scAAV9-mCMV-hIDS delivery at an effective dose can not only slow down but also halt the progression of MPS II, depending on the age of treatment. Our minimally efficacious vector dose was as low as  $2.5 \times 10^{12}$  vg/kg for scAAV9-mCMV-hIDS delivered via the systemic route. An i.v. injection of  $2.5 \times 10^{12}$  vg/kg and  $5 \times 10^{12}$  vg/kg scAAV9-mCMV-hIDS in MPS II mice at age 1 month or  $5 \times 10^{12}$  to  $2 \times 10^{13}$  vg/kg at age 6 months led to the effective restoration of



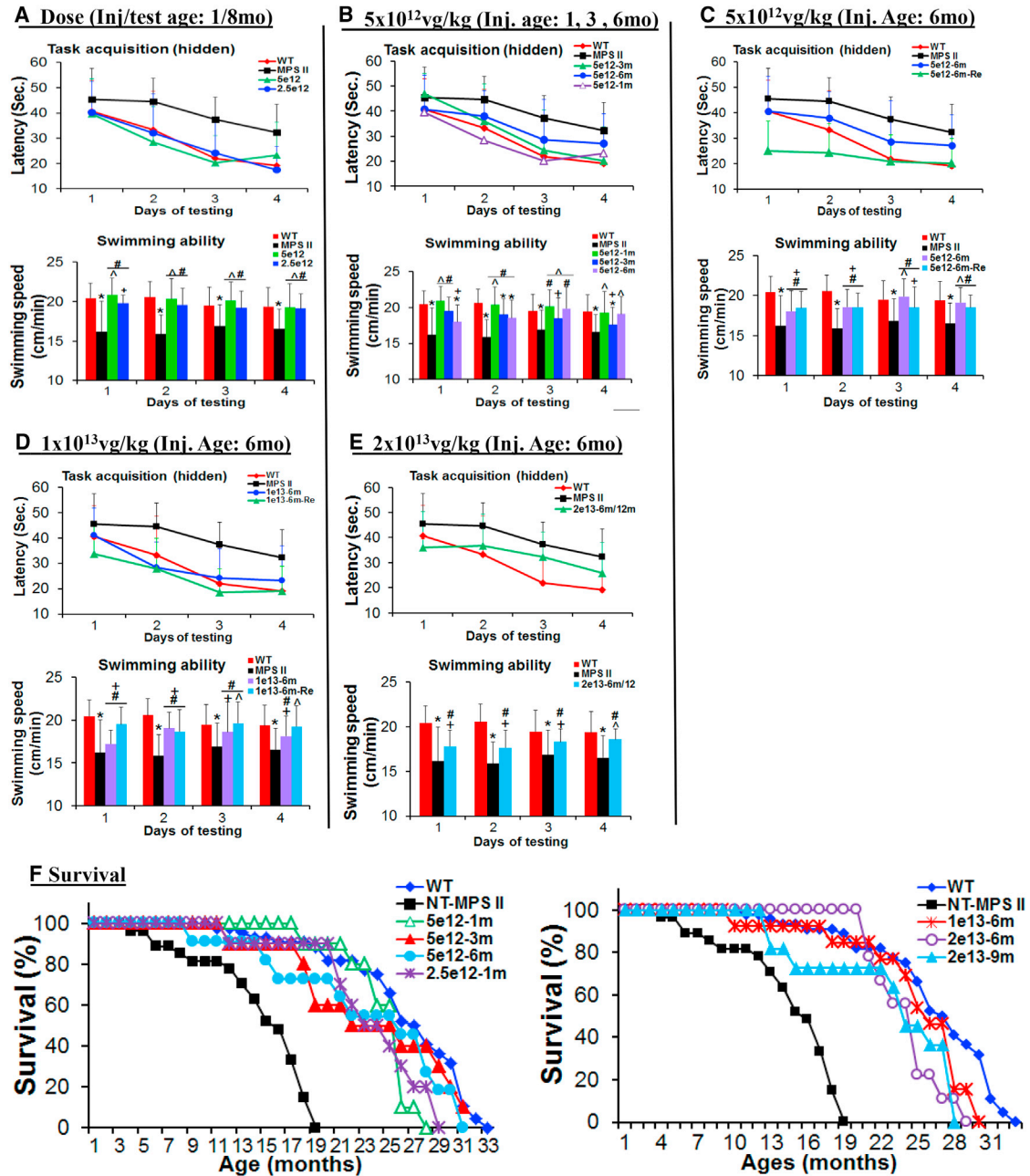


**Figure 5. Significant Improvement in Behavior Performance and Survival after a Systemic sCAAV9-mCMV-hIDS Gene Delivery**

(A–E) MPS II mice were treated at age 1 month, 3 months, 6 months, or 9 months with an i.v. injection of sCAAV9-mCMV-hIDS at (A–C)  $5 \times 10^{12}$  vg/kg, (D)  $1 \times 10^{13}$  vg/kg, or (E)  $2 \times 10^{13}$  vg/kg. Behavior testing was performed in a hidden task in the Morris water maze when they were 8 months and/or 12 months old (-Re). (A) Dose comparison. (B) Comparison of treatment ages. (C–E) Vector treatment at age 6 months; (C)  $5 \times 10^{12}$  vg/kg, (D)  $1 \times 10^{13}$  vg/kg, and (E)  $2 \times 10^{13}$  vg/kg. Data were means  $\pm$  SD of latency to find hidden platform (in seconds) and swimming speed (in centimeters per second). \* $p < 0.05$  versus WT;  $\wedge p > 0.05$  versus WT; # $p < 0.05$  versus non-treated MPS II; + $p > 0.05$  versus non-treated MPS II.

(F) Survival.

functional IDS expression in the brain and all seven tested somatic tissues, which were sufficient to result in the clearance of lysosomal GAG storage to the endpoint, correction of cognitive and motor func-

tions, and extension of survival to mostly within the normal range of lifespan. Importantly, treatment at age 9 months with  $2 \times 10^{13}$  vg/kg vector also led to the extended survival in the majority of MPS II mice



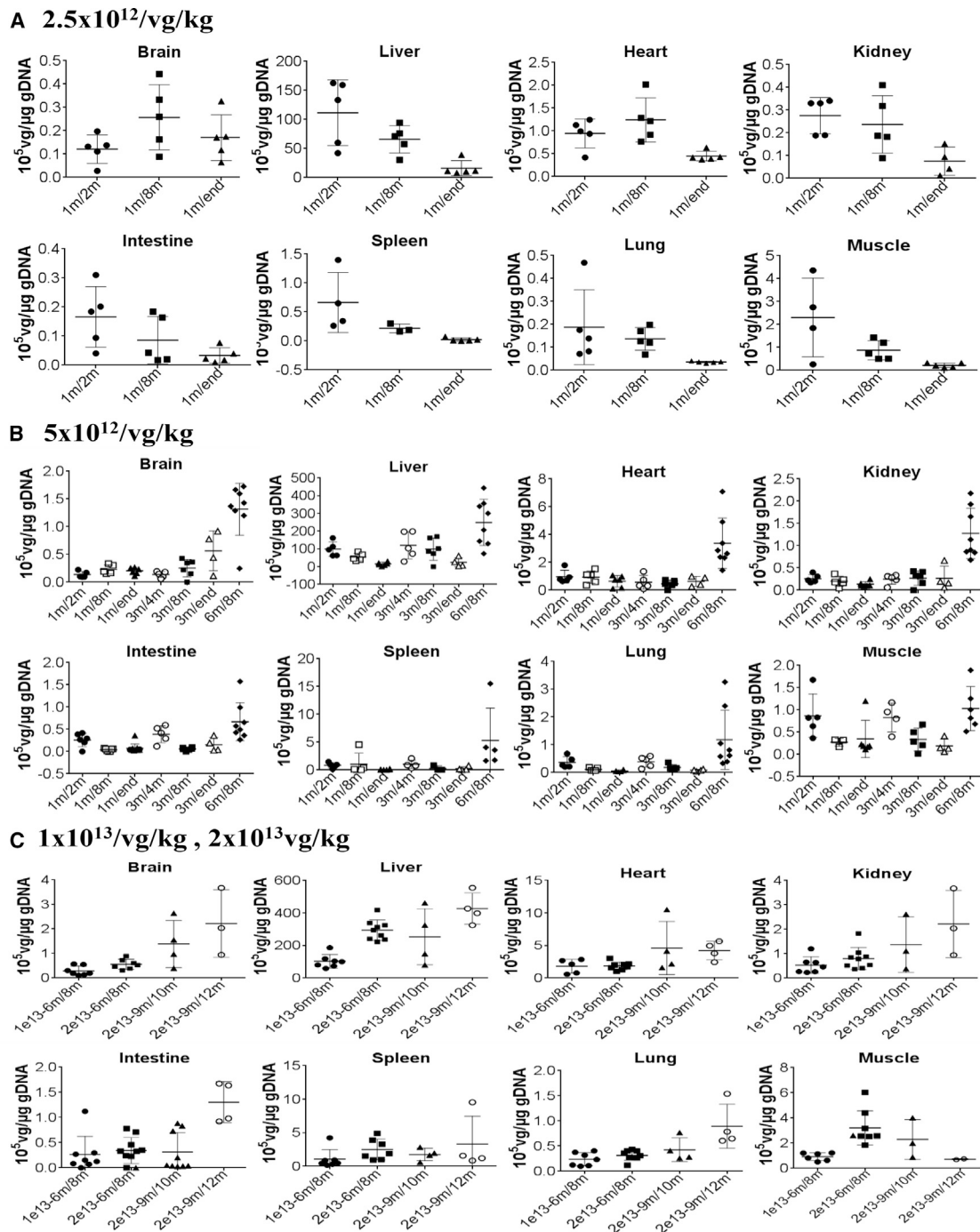


**Figure 6. Differential Biodistribution of Systemically Delivered scAAV9-mCMV-hDS Vector in MPS II Mice**

(A–C) MPS II mice were treated with an i.v. injection of (A)  $2.5 \times 10^{12}$  vg/kg, (B)  $5 \times 10^{12}$  vg/kg, (C)  $1 \times 10^{13}$  vg/kg, or  $2 \times 10^{13}$  vg/kg scAAV9-mCMV-hDS at different ages. Tissues were assayed by qPCR for scAAV9-hDS vector genome at different time points post-vector treatment ( $n = 5$  per group). m/m, injection age/testing age. Data expressed as  $10^5$  vg/ $\mu$ g gDNA. Vector genome was detected at  $<0.005 \times 10^5$  vg/ $\mu$ g gDNA in non-treated WT and MPS II mice ( $n = 12$  per group).

with the clearance of GAG storage, though behavior data were not available due to the lack of matched controls. Notably, 9 months is an age by which significant neuropathology and somatic disorders

have taken place, and some of the untreated MPS II mice have either died or reached the humane endpoint. Interestingly, while there was no clear correlation between tissue rIDS levels and vg copies,

**Table 2. Tumor Incidence in AAV9-Treated MPS II and Non-treated WT Mice**

Mice	Vector Dose (vg/kg)	Injection Age (Months)	Test Age (Months)	No. of Mice			p Value <sup>b</sup>
				Necropsy	Tumors <sup>a</sup>	Tumor Rate (%)	
WT	N/A	N/A	14.7–30.7	25	9	36	–
MPS II	$2.5 \times 10^{12}$	1	20.1–29.4	7	4	57	0.314
	$5 \times 10^{12}$	1	16.3–27.5	7	4	57	0.314
	$5 \times 10^{12}$	3	17.7–29.2	5	2	20	0.865
	$5 \times 10^{12}$	6	15.0–29.4	7	1	14	0.273
	$1 \times 10^{13}$	6	16.0–25.8	7	3	43	0.740
	$2 \times 10^{13}$	6	20.7–24.4	5	1	20	0.488
	$2 \times 10^{13}$	9	13.2–23.7	4	1	25	0.667
Total	–	–	–	42	16	38.1	0.864

N/A, not applicable.  
<sup>a</sup>Gross and/or microscopic tumors.  
<sup>b</sup>p value versus WT rate by chi-square analysis.

tissue GAG contents in all vector-treated MPS II mice were reduced to levels comparable to those in WT mice until the endpoint, suggesting effective correction and reversal of GAG storage in both the CNS and somatic tissues, despite the age at vector delivery and the variation in tissue rIDS levels. This indicates that a systemic delivery of scAAV9-mCMV-hIDS at an effective dose can mediate the expression of functional rIDS at levels sufficient to effectively clear CNS and somatic GAG storage, regardless of the disease stage to a certain extent, offering extended clinical potential for treating MPS II in humans. Notably, our previous study showed that treating MPS IIIA mice at age 9 months with scAAV9-U1a-hSGSH provided only minimal functional benefit, with no improvement in survival.<sup>41</sup> It is unclear why this scAAV9-hIDS for MPS II is more effective in reversing the disease than scAAV9-hGSH for MPS IIIA. However, it is known that the premature death in MPS II is attributed to not only neuropathy but also severe pulmonary and cardiac manifestations, while mortality in MPS IIIA was predominantly due to neurological manifestation. Therefore, it is likely that this expanded functional therapeutic benefit of scAAV9-hIDS for MPS II is the consequence of the neurological benefits enhanced with somatic correction.

While achieving effective global CNS and widespread somatic transduction as expected, this study demonstrates the extended neurological potential of systemic scAAV9-mCMV-hIDS gene delivery for the treatment of MPS II, similar to that observed in MPS IIIA mice treated with scAAV9-U1a-hSGSH.<sup>41</sup> It was also evident that the vector treatment led to the clearance of lysosomal storage pathology and the correction of gliosis in the enteric nervous system and in retina, indicating effective correction of lysosomal storage pathology and gliosis in the PNS and ONS in the vector-treated MPS II mice. These are clinically relevant, because neuropathologies affect the entire nervous system, including the CNS, PNS, and ONS, and retinopathies—including retinal degeneration—are common in all neuro-pathic MPS disorders, including MPS II.<sup>42,43</sup> These observations

highlight the potential for added, therapeutically meaningful, benefits from the systemic gene delivery approach in this disease, with which the majority of patients are manifested with both severe significant somatic disorders and profound CNS neurodegeneration.

Furthermore, in this study, an i.v. scAAV9-mCMV-hIDS delivery also led to the clearance of lysosomal storage in non-neuronal tissues of eye in MPS II mice, including cornea, iris, and ciliary process. These are important clinically meaningful findings, further supporting the ever-expanded clinical potentials of systemic scAAV9 gene delivery targeting the root cause for the treatment of MPS II, other neuropathic LSDs, and other neurogenetic diseases. Our data also indicate the need of further investigating the tissue tropism of AAV9 and other AAV serotypes to better understand their therapeutic potential as gene therapy vectors.

Notably, at humane endpoints, tumors were observed in the liver at similar incidences (35.7% versus 36%) in scAAV9-hIDS-treated MPS II mice (ages 16–25 months) and non-treated WT mice (ages 23–29 months). The observed tumor incidences in the vector-treated MPS II mice were not dose dependent, while higher but insignificant tumor incidence was observed in mice treated at age 1 month than in mice treated at age 6 months. We, therefore, believe that the tumor incidences in vector-treated mice are largely due to aging, given the normalized or close to normalized survival in MPS II mice that received the vector treatment. Furthermore, while the vg was detected in tumors, suggesting the potential of the vector integration, this study indicates that the systemic delivery of scAAV9-mCMV-hIDS does not pose significant risk of tumorigenicity or any specific risk of genotoxicity, given that the observed tumor incidences were very similar between the vector-treated MPS II mice and non-treated WT mice. In addition, the systemic scAAV9-mCMV-hIDS gene delivery did not result in observable adverse events or detectable systemic toxicity in MPS II mice. This, along with the low incidence of tumors in treated MPS II mice compared to non-treated WT mice,

supports a generally safe profile of systemic scAAV9-mCMV-hIDS vector delivery in MPS II mice.

In summary, we have generated a safe and effective self-complementary rAAV9-hIDS gene delivery approach for the treatment of MPS II. The comprehensive preclinical study results reinforce the view that systemic delivery of the *trans*-BBB-neurotropic AAV9 gene therapy vector can prevent and reverse the global neuropathy and broad somatic manifestations of the disease. This study promises an effective and minimally invasive gene therapy approach for treating MPS II in patients. Notably, the results of this study have led to the recent IND approval by the FDA for a phase 1/2 clinical trial of systemic scAAV9-mCMV-hIDS gene delivery in patients with MPS II (IND #17838). Once again, this study further demonstrates the great potential of the demonstrated systemic AAV9 gene delivery platform for the effective translation of rAAV9 gene therapy products to clinical application to benefit broad populations of patients.

## MATERIALS AND METHODS

### Animals

The knockout mouse model of MPS II (B6N.Cg-IDS<sup>tm1Muen/J</sup>) was developed by disrupting exons 4 and 5 of the murine IDS gene using homologous recombination.<sup>44,45</sup> The MPS II mouse colony was maintained on a C57BL/6 background by backcrosses of female heterozygotes with C57BL/6 males in the vivarium at the Research Institute at Nationwide Children's Hospital (NCH-RI). The genotypes of progeny mice were identified by PCR.<sup>44</sup> MPS II mice resemble the human disease in virtually all aspects, including X-linked inheritance pattern. All MPS II mice are male that have no detectable IDS activity and exhibit phenotypes corresponding to severe-form MPS II in humans, with characteristic lysosomal storage pathology in cells of virtually all organs, progressive profound neurological and severe somatic manifestations, and a significantly shortened lifespan. All animal care and procedures were performed strictly following the approved protocol (Institutional Animal Care and Use Committee [IACUC], NCH-RI), in accordance with the Guide for the Care and Use of Laboratory Animals (8th edition). MPS II mice (all male) and their age-matched WT male littermates were used in the experiments.

### Recombinant AAV Viral Vector

A scAAV vector plasmid was constructed to produce scAAV9-mCMV-hIDS viral vector (Figure S1). The vg contains minimal elements for transgene expression, including a WT AAV2 terminal repeat (ITR), an AAV2 terminal repeat with deletion of the terminal resolution site to force generation of self-complementary dimeric genomes (dITR), a truncated 173-bp mini-CMV (mCMV) promoter, human IDS coding sequence (hIDS), and simian virus 40 (SV40) polyadenylation signal. The scAAV9-mCMV-hIDS viral vectors were manufactured by NCH Viral Vector Core (NCH-VVC) and SAB Tech. The viral vectors were produced in HEK293 cells using three-plasmid co-transfection and purified by cation exchange column chromatography (NCH-VVC) or CsCl gradient centrifugation (SAB Tech), and dialysis into Tris-buffered saline (TBS; pH 8.0).

For dosing, the vector titer was determined by dot-blot hybridization using the hIDS coding sequence as probe and serially diluted linearized AAV-mCMV-hIDS plasmid as standard.

### Systemic Vector Delivery

MPS II mice (all male) were treated at different ages and at different doses with an i.v. injection of scAAV9-mCMV-hIDS vector (in 150–200  $\mu$ L saline) via tail vein. Age- and sex-matched saline-injected MPS II and WT littermates were used as controls.

### Behavioral Tests: Hidden Task in the Morris Water Maze

The scAAV9-mCMV-hIDS-treated MPS II mice and controls were tested for behavioral performance approximately at age 8 months and/or 12 months in a hidden task in the Morris water maze.<sup>46</sup> The water maze consisted of a large circular pool (diameter, 122 cm) filled with water (45 cm deep, 24°C–26°C) containing 1% white tempera paint, located in a room with numerous visual cues. Mice were tested for their ability to find a hidden escape platform (20  $\times$  20 cm) 0.5 cm under the water surface. Each animal was given four trials per day across 4 days. For each trial, the mouse was placed in the pool at one of four randomly ordered locations and then given 60 s to swim to the hidden platform. If the mouse found the platform, the trial ended, and the animal was allowed to remain for 10 s on the platform before the next trial began. If the platform was not found within 60 s, the mouse was placed on the platform for 10 s and then given the next trial. Measures were taken of latency to find the platform (in seconds), and swimming speed (in centimeters per second) through an automated tracking system (San Diego Instruments, San Diego, CA, USA).

### Longevity Observation

Following the scAAV9-mCMV-hIDS vector injection, subsets of mice were continuously observed for the development of humane endpoint criteria or until death occurred. The endpoint was when the symptoms of late-stage MPS II clinical manifestation (urine retention, rectal prolapse, protruding penis) became irreversible or when mice showed significant weight loss, dehydration, or morbidity.

### Necropsy and Tissue Analyses

Necropsies were carried out when mice were at different times pi of vector and at the humane endpoint. Brain and multiple somatic tissues were collected and stored either at  $-80^{\circ}\text{C}$  or in 4% paraformaldehyde (in PBS; pH 7.2) before being processed for analyses. Observations were performed at necropsy to detect gross tissue abnormalities.

### IDS Activity Assay

Tissue samples were assayed for IDS enzyme activity following previously published procedures.<sup>47</sup> The assay measures 4-methylumbelliferone (4MU), a fluorochrome formed by 2-step sequential action of IDS and  $\alpha$ -iduronidase on the substrate 4-methylumbelliferyl- $\alpha$ -iduronate-2-sulfate (a kind gift from Dr. Michael Gelb, University of Washington). The sample IDS activity desulfates the substrate over a 4-hr reaction at 37°C, followed by a secondary enzymatic reaction



with excess  $\alpha$ -iduronidase (Aldurazyme, BioMarin), releasing the 4MU fluorescent product over 24 hr at 37°C. The IDS activity is expressed as units per milligram of protein. One unit is equal to 1 nmol 4MU released per hour.

#### GAG Content Measurement

GAGs were extracted from wet tissues following published procedures with modification.<sup>20,48</sup> A dimethylmethylene blue (DMB) assay was used to measure GAG content.<sup>49</sup> The GAG samples from 1.0 mg tissue were mixed with H<sub>2</sub>O to 40  $\mu$ L before adding 35 nM DMB (Polysciences, Warrington, PA, USA) in 0.2M sodium formate buffer (pH 3.5). The product was measured using a spectrophotometer (optical density 535; OD<sub>535</sub>). The GAG content was expressed as micrograms per milligram of tissue.

#### IF

Tissues were processed for thin paraffin sections (4  $\mu$ m) and IF. The IF staining was performed for astrocytes or lysosomal signals, using antibodies against GFAP (Millipore) or LAMP1 (Abcam) and corresponding secondary antibody conjugated with Alexa Fluor 568 or Alexa Fluor 488 (Invitrogen), following procedures recommended by the manufacturers. The sections were imaged under a fluorescence microscope.

#### Real-Time qPCR

Total DNA was isolated from tissue samples of scAAV9-treated and non-treated mice using QIAGEN DNeasy columns. The DNA samples were analyzed by qPCR, using Absolute Blue QPCR Mix (Thermo Scientific) and the Applied Biosystems 7000 Real-Time PCR System, following the procedures recommended by the manufacturer. TaqMan primers and probes specific for mCMV were used to detect rAAV vg: forward: 5'-GGCCCGCCTGG CTGAC-3'; reverse: 5'-GTGCCAAAACAACTCCCATTG-3'; probe: 5'-[6-FAM] AACGACCCCGGACTCACGG [BHQ1a~6FAM]-3'. gDNA was quantified in parallel samples using  $\beta$ -actin-specific primers: forward: 5'-GTCATCACTATTGGC AACGA-3'; reverse: 5'-CTCAGG AGTTTTGTACCTT-3'; probe: 5'-[6-FAM]TTCCGATGCCCTGAGGCTCT[BHQ1a~6FAM]-3'. Genomic DNA from tissues of non-treated mice was used as control for background levels and absence of contamination. Data are expressed as 10<sup>5</sup> vg/ $\mu$ g gDNA.

#### Histopathology

Paraffin sections (4  $\mu$ m) of brain and multiple somatic tissues were processed for H&E staining by the Morphology Core in the Research Institute at Nationwide Children's Hospital. The sections were examined by a board-certified veterinary pathologist at GEMpath (Longmont, CO, USA).

#### Statistics

Data were analyzed using Student's t test and/or separate one-way ANOVAs to examine group differences. For all comparisons, significance was set at  $p \leq 0.05$ .

#### SUPPLEMENTAL INFORMATION

Supplemental Information includes two figures and one table and can be found with this article online at <https://doi.org/10.1016/j.omtm.2018.07.005>.

#### AUTHOR CONTRIBUTIONS

H.F. designed the studies, obtained funding, performed data analyses, and wrote the manuscript. K.Z. performed the experiments, vector testing, tissue analyses, data collection, and data analyses. N.M. performed vector testing, tissue analyses, and data collection. A.S.M. and R.J.P. conducted tissue analyses and data collection. D.M.M. co-designed the studies, obtained funding, performed data analyses, and co-wrote the manuscript. J.M. co-designed the studies, obtained funding and revised the manuscript.

#### CONFLICTS OF INTEREST

J.M. is a consultant for Shire, a principal investigator (PI) for Shire intrathecal ERT studies for MPS II, and a PI for a Sangamo phase I/II gene editing clinical trial for MPS II. The remaining authors declare no conflict of interest.

#### ACKNOWLEDGMENTS

This study was supported by funds from friends and families of MPS II patients through Project Alive (previously the Hunter Syndrome Research Coalition), the Canadian MPS Society, The Isaac Foundation (Canada), the Caring for Carter Foundation/National MPS Society, the Hunter Syndrome Foundation, and the Sock-it 2 Hunter Syndrome Foundation.

#### REFERENCES

- Neufeld, E.F., and Muenzer, J. (2014). *The Mucopolysaccharidoses* (The McGraw-Hill Companies).
- Bradley, L.A., Haddow, H.R.M., and Palomaki, G.E. (2017). Treatment of mucopolysaccharidosis type II (Hunter syndrome): results from a systematic evidence review. *Genet. Med.* *19*, 1187–1201.
- Muenzer, J., Hendriksz, C.J., Fan, Z., Vijayaraghavan, S., Perry, V., Santra, S., Solanki, G.A., Mascelli, M.A., Pan, L., Wang, N., et al. (2016). A phase I/II study of intrathecal idursulfase-IT in children with severe mucopolysaccharidosis II. *Genet. Med.* *18*, 73–81.
- Sands, M.S., and Davidson, B.L. (2006). Gene therapy for lysosomal storage diseases. *Mol. Ther.* *13*, 839–849.
- Daya, S., and Berns, K.I. (2008). Gene therapy using adeno-associated virus vectors. *Clin. Microbiol. Rev.* *21*, 583–593.
- Zincarelli, C., Soltys, S., Rengo, G., and Rabinowitz, J.E. (2008). Analysis of AAV serotypes 1–9 mediated gene expression and tropism in mice after systemic injection. *Mol. Ther.* *16*, 1073–1080.
- Samulski, R.J., Chang, L.S., and Shenk, T. (1987). A recombinant plasmid from which an infectious adeno-associated virus genome can be excised in vitro and its use to study viral replication. *J. Virol.* *61*, 3096–3101.
- Berns, K.I., and Linden, R.M. (1995). The cryptic life style of adeno-associated virus. *BioEssays* *17*, 237–245.
- McPhee, S.W., Janson, C.G., Li, C., Samulski, R.J., Camp, A.S., Francis, J., Shera, D., Liouthermann, L., Feely, M., Freese, A., and Leone, P. (2006). Immune responses to AAV in a phase I study for Canavan disease. *J. Gene Med.* *8*, 577–588.
- Daadi, M.M., Pivrotto, P., Bringas, J., Cunningham, J., Forsayeth, J., Eberling, J., and Bankiewicz, K.S. (2006). Distribution of AAV2-hAADC-transduced cells after 3 years in Parkinsonian monkeys. *Neuroreport* *17*, 201–204.

11. Desmaris, N., Verot, L., Puech, J.P., Caillaud, C., Vanier, M.T., and Heard, J.M. (2004). Prevention of neuropathology in the mouse model of Hurler syndrome. *Ann. Neurol.* 56, 68–76.
12. Fu, H., Samulski, R.J., McCown, T.J., Picornell, Y.J., Fletcher, D., and Muenzer, J. (2002). Neurological correction of lysosomal storage in a mucopolysaccharidosis IIIB mouse model by adeno-associated virus-mediated gene delivery. *Mol. Ther.* 5, 42–49.
13. Cressant, A., Desmaris, N., Verot, L., Bréjot, T., Froissart, R., Vanier, M.T., Maire, I., and Heard, J.M. (2004). Improved behavior and neuropathology in the mouse model of Sanfilippo type IIIB disease after adeno-associated virus-mediated gene transfer in the striatum. *J. Neurosci.* 24, 10229–10239.
14. Elliger, S.S., Elliger, C.A., Aguilar, C.P., Raju, N.R., and Watson, G.L. (1999). Elimination of lysosomal storage in brains of MPS VII mice treated by intrathecal administration of an adeno-associated virus vector. *Gene Ther.* 6, 1175–1178.
15. Passini, M.A., Watson, D.J., Vite, C.H., Landsburg, D.J., Feigenbaum, A.L., and Wolfe, J.H. (2003). Intraventricular brain injection of adeno-associated virus type 1 (AAV1) in neonatal mice results in complementary patterns of neuronal transduction to AAV2 and total long-term correction of storage lesions in the brains of beta-glucuronidase-deficient mice. *J. Virol.* 77, 7034–7040.
16. Hackett, N.R., Redmond, D.E., Sondhi, D., Giannaris, E.L., Vassallo, E., Stratton, J., Qiu, J., Kaminsky, S.M., Lesser, M.L., Fisch, G.S., et al. (2005). Safety of direct administration of AAV2(CU)hCLN2, a candidate treatment for the central nervous system manifestations of late infantile neuronal ceroid lipofuscinosis, to the brain of rats and nonhuman primates. *Hum. Gene Ther.* 16, 1484–1503.
17. Tardieu, M., Zerah, M., Husson, B., de Bournonville, S., Deiva, K., Adamsbaum, C., Vincent, F., Hocquemiller, M., Broissand, C., Furlan, V., et al. (2014). Intracerebral administration of adeno-associated viral vector serotype rh.10 carrying human SGSH and SUMF1 cDNAs in children with mucopolysaccharidosis type IIIA disease: results of a phase I/II trial. *Hum. Gene Ther.* 25, 506–516.
18. Fu, H., Muenzer, J., Samulski, R.J., Breese, G., Sifford, J., Zeng, X., and McCarty, D.M. (2003). Self-complementary adeno-associated virus serotype 2 vector: global distribution and broad dispersion of AAV-mediated transgene expression in mouse brain. *Mol. Ther.* 8, 911–917.
19. McCarty, D.M., DiRosario, J., Gulaid, K., Muenzer, J., and Fu, H. (2009). Mannitol-facilitated CNS entry of rAAV2 vector significantly delayed the neurological disease progression in MPS IIIB mice. *Gene Ther.* 16, 1340–1352.
20. Fu, H., Kang, L., Jennings, J.S., Moy, S.S., Perez, A., Dirosario, J., McCarty, D.M., and Muenzer, J. (2007). Significantly increased lifespan and improved behavioral performances by rAAV gene delivery in adult mucopolysaccharidosis IIIB mice. *Gene Ther.* 14, 1065–1077.
21. Foust, K.D., Nurre, E., Montgomery, C.L., Hernandez, A., Chan, C.M., and Kaspar, B.K. (2009). Intravascular AAV9 preferentially targets neonatal neurons and adult astrocytes. *Nat. Biotechnol.* 27, 59–65.
22. Duque, S., Joussemet, B., Riviere, C., Marais, T., Dubreil, L., Douar, A.M., Fyfe, J., Moullier, P., Colle, M.A., and Barkats, M. (2009). Intravenous administration of self-complementary AAV9 enables transgene delivery to adult motor neurons. *Mol. Ther.* 17, 1187–1196.
23. Bevan, A.K., Duque, S., Foust, K.D., Morales, P.R., Braun, L., Schmelzer, L., Chan, C.M., McCrate, M., Chicoine, L.G., Coley, B.D., et al. (2011). Systemic gene delivery in large species for targeting spinal cord, brain, and peripheral tissues for pediatric disorders. *Mol. Ther.* 19, 1971–1980.
24. Fu, H., Dirosario, J., Killeard, S., Zaraspe, K., and McCarty, D.M. (2011). Correction of neurological disease of mucopolysaccharidosis IIIB in adult mice by rAAV9 trans-blood-brain barrier gene delivery. *Mol. Ther.* 19, 1025–1033.
25. Ruza, A., Marcó, S., García, M., Villacampa, P., Ribera, A., Ayuso, E., Maggioni, L., Mingozzi, F., Haurigot, B., and Bosch, F. (2012). Correction of pathological accumulation of glycosaminoglycans in central nervous system and peripheral tissues of MPSIIIA mice through systemic AAV9 gene transfer. *Hum. Gene Ther.* 23, 1237–1246.
26. Weismann, C.M., Ferreira, J., Keeler, A.M., Su, Q., Qui, L., Shaffer, S.A., Xu, Z., Gao, G., and Sena-Esteves, M. (2015). Systemic AAV9 gene transfer in adult GM1 gangliosidosis mice reduces lysosomal storage in CNS and extends lifespan. *Hum. Mol. Genet.* 24, 4353–4364.
27. Gurda, B.L., De Guilhem De Lataillade, A., Bell, P., Zhu, Y., Yu, H., Wang, P., Bagel, J., Vite, C.H., Sikora, T., Hinderer, C., et al. (2016). Evaluation of AAV-mediated gene therapy for central nervous system disease in canine mucopolysaccharidosis VII. *Mol. Ther.* 24, 206–216.
28. Lee, N.C., Muramatsu, S., Chien, Y.H., Liu, W.S., Wang, W.H., Cheng, C.H., Hu, M.K., Chen, P.W., Tzen, K.Y., Byrne, B.J., and Hwu, W.L. (2015). Benefits of neuronal preferential systemic gene therapy for neurotransmitter deficiency. *Mol. Ther.* 23, 1572–1581.
29. Murrey, D.A., Naughton, B.J., Duncan, F.J., Meadows, A.S., Ware, T.A., Campbell, K.J., Bremer, W.G., Walker, C.M., Goodchild, L., Bolon, B., et al. (2014). Feasibility and safety of systemic rAAV9-hNAGLU delivery for treating mucopolysaccharidosis IIIB: toxicology, biodistribution, and immunological assessments in primates. *Hum. Gene Ther. Clin. Dev.* 25, 72–84.
30. Meadows, A.S., Duncan, F.J., Camboni, M., Waligura, K., Montgomery, C., Zaraspe, K., Naughton, B.J., Bremer, W.G., Shilling, C., Walker, C.M., et al. (2015). A GLP-compliant toxicology and biodistribution study: systemic delivery of an rAAV9 vector for the treatment of mucopolysaccharidosis IIIB. *Hum. Gene Ther. Clin. Dev.* 26, 228–242.
31. Haurigot, V., and Bosch, F. (2013). Toward a gene therapy for neurological and somatic MPSIIIA. *Rare Dis.* 1, e27209.
32. Hinderer, C., Bell, P., Gurda, B.L., Wang, Q., Louboutin, J.P., Zhu, Y., Bagel, J., O'Donnell, P., Sikora, T., Ruane, T., et al. (2014). Intrathecal gene therapy corrects CNS pathology in a feline model of mucopolysaccharidosis I. *Mol. Ther.* 22, 2018–2027.
33. Ribera, A., Haurigot, V., Garcia, M., Marcó, S., Motas, S., Villacampa, P., Maggioni, L., León, X., Molas, M., Sánchez, V., et al. (2015). Biochemical, histological and functional correction of mucopolysaccharidosis type IIIB by intra-cerebrospinal fluid gene therapy. *Hum. Mol. Genet.* 24, 2078–2095.
34. Duque, S.I., Arnold, W.D., Odermatt, P., Li, X., Porensky, P.N., Schmelzer, L., Meyer, K., Kolb, S.J., Schümperli, D., Kaspar, B.K., and Burghes, A.H. (2015). A large animal model of spinal muscular atrophy and correction of phenotype. *Ann. Neurol.* 77, 399–414.
35. Meyer, K., Ferraiuolo, L., Schmelzer, L., Braun, L., McGovern, V., Likhite, S., Michels, O., Govoni, A., Fitzgerald, J., Morales, P., et al. (2015). Improving single injection CSF delivery of AAV9-mediated gene therapy for SMA: a dose-response study in mice and nonhuman primates. *Mol. Ther.* 23, 477–487.
36. Mussche, S., Devreese, B., Nagabhushan Kalburgi, S., Bachaboina, L., Fox, J.C., Shih, H.J., Van Coster, R., Samulski, R.J., and Gray, S.J. (2013). Restoration of cytoskeleton homeostasis after gigaxonin gene transfer for giant axonal neuropathy. *Hum. Gene Ther.* 24, 209–219.
37. Hinderer, C., Katz, N., Louboutin, J.P., Bell, P., Yu, H., Nayal, M., Kozarsky, K., O'Brien, W.T., Goode, T., and Wilson, J.M. (2016). Delivery of an adeno-associated virus vector into cerebrospinal fluid attenuates central nervous system disease in mucopolysaccharidosis type II mice. *Hum. Gene Ther.* 27, 906–915.
38. Motas, S., Haurigot, V., Garcia, M., Marcó, S., Ribera, A., Roca, C., Sánchez, X., Sánchez, V., Molas, M., Bertolin, J., et al. (2016). CNS-directed gene therapy for the treatment of neurologic and somatic mucopolysaccharidosis type II (Hunter syndrome). *JCI Insight* 1, e86696.
39. Sharma, R., Anguela, X.M., Doyon, Y., Wechsler, T., DeKelver, R.C., Sproul, S., Paschon, D.E., Miller, J.C., Davidson, R.J., Shivak, D., et al. (2015). In vivo genome editing of the albumin locus as a platform for protein replacement therapy. *Blood* 126, 1777–1784.
40. Ferla, R., O'Malley, T., Calcedo, R., O'Donnell, P., Wang, P., Cotugno, G., Claudiani, P., Wilson, J.M., Haskins, M., and Auricchio, A. (2013). Gene therapy for mucopolysaccharidosis type VI is effective in cats without pre-existing immunity to AAV8. *Hum. Gene Ther.* 24, 163–169.
41. Fu, H., Cataldi, M.P., Ware, T.A., Zaraspe, K., Meadows, A.S., Murrey, D.A., and McCarty, D.M. (2016). Functional correction of neurological and somatic disorders at later stages of disease in MPS IIIA mice by systemic scAAV9-hSGSH gene delivery. *Mol. Ther. Methods Clin. Dev.* 3, 16036.
42. Summers, C.G., and Ashworth, J.L. (2011). Ocular manifestations as key features for diagnosing mucopolysaccharidoses. *Rheumatology (Oxford)* 50 (Suppl 5), v34–v40.

43. Ashworth, J.L., Biswas, S., Wraith, E., and Lloyd, I.C. (2006). The ocular features of the mucopolysaccharidoses. *Eye (Lond.)* 20, 553–563.
44. Muenzer, J., and Fu, H. (1999). Targeted disruption of the mouse iduronate sulfatase gene. *Am. J. Hum. Genet.* 65, A427.
45. Garcia, A.R., Pan, J., Lamsa, J.C., and Muenzer, J. (2007). The characterization of a murine model of mucopolysaccharidosis II (Hunter syndrome). *J. Inherit. Metab. Dis.* 30, 924–934.
46. Warburton, E.C., Baird, A., Morgan, A., Muir, J.L., and Aggleton, J.P. (2001). The conjoint importance of the hippocampus and anterior thalamic nuclei for allocentric spatial learning: evidence from a disconnection study in the rat. *J. Neurosci.* 21, 7323–7330.
47. Voznyi, Y.V., Keulemans, J.L., and van Diggelen, O.P. (2001). A fluorimetric enzyme assay for the diagnosis of MPS II (Hunter disease). *J. Inherit. Metab. Dis.* 24, 675–680.
48. van de Lest, C.H., Versteeg, E.M., Veerkamp, J.H., and van Kuppevelt, T.H. (1994). Quantification and characterization of glycosaminoglycans at the nanogram level by a combined azure A-silver staining in agarose gels. *Anal. Biochem.* 221, 356–361.
49. de Jong, J.G., Wevers, R.A., Laarakkers, C., and Poorthuis, B.J. (1989). Dimethylmethylene blue-based spectrophotometry of glycosaminoglycans in untreated urine: a rapid screening procedure for mucopolysaccharidoses. *Clin. Chem.* 35, 1472–1477.



OMTM, Volume 10

## **Supplemental Information**

**Targeting Root Cause by Systemic scAAV9-hIDS**

**Gene Delivery: Functional Correction**

**and Reversal of Severe MPS II in Mice**

**Haiyan Fu, Kim Zaraspe, Naoko Murakami, Aaron S. Meadows, Ricardo J. Pineda, Douglas M. McCarty, and Joseph Muenzer**

**Figure S1**

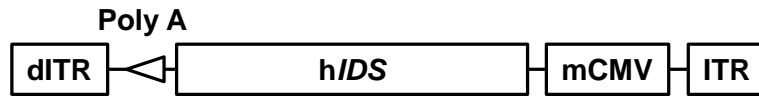
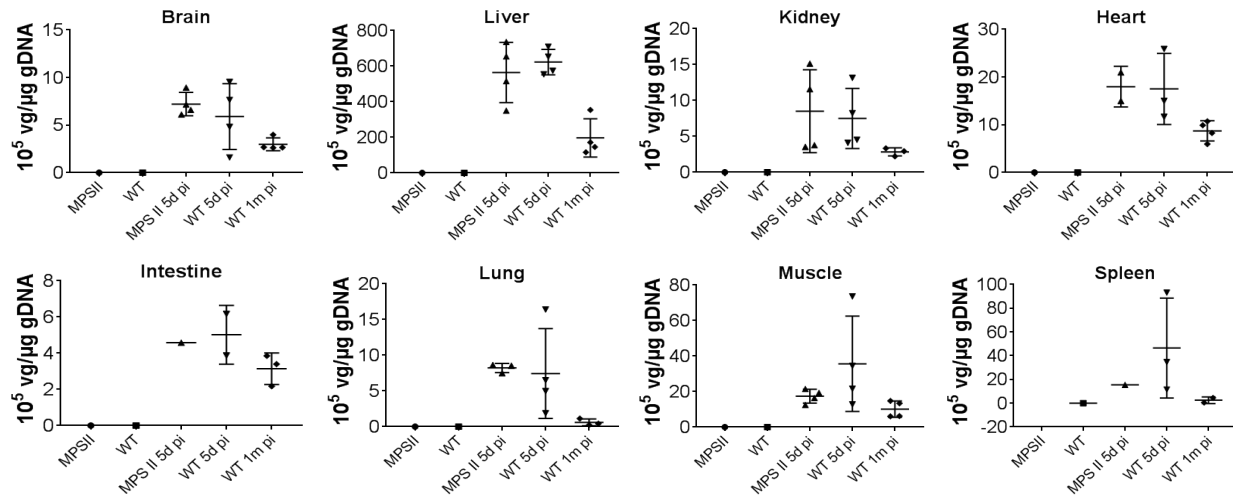


**Figure S1. scAAV9-mCMV-hIDS vector genome. ITR:** wt AAV2 terminal repeat; **dITR:** AAV2 terminal repeat with deletion of terminal resolution site to force generation of self-complementary dimeric genomes; **mCMV:** a truncated 173bp mini CMV promoter; **hIDS:** human iduronate sulfatase coding region cDNA; **Poly A:** SV40 polyadenylation signal.

## Supplementary Figure S2



**Supplementary Figure S2 Differential biodistribution of systemically delivered scAAV9-mCMV-hIDS vector in MPS II and WT mice.** MPS II and WT mice were treated at age 1-2m with an IV injection of  $5 \times 10^{13}$  vg/kg scAAV9-mCMV-hIDS. Tissues were assayed by qPCR for scAAV9-hIDS vector genome at 5 days or 1m pi (n=4/group).



Table S1. Tumor incidence in AAV9-treated MPS II and non-treated WT mice at endpoints							
Mouse ID #	GT	Vector dose (vg/kg)	Injection age (m)	Test age (m)	Tumors		10 <sup>5</sup> vg/ $\mu$ g gDNA
					Gross	Microscopic <sup>#</sup>	
855	MPS II	2.5x10 <sup>12</sup>	1	20	Liver	ND*	0.405 (T1) 6.850 (T2)
858	MPS II	2.5x10 <sup>12</sup>	1	21	Liver	ND*	0.366 (T1) 9.550 (T2) 0.021 (T3)
870	MPS II	2.5x10 <sup>12</sup>	1	26	Liver	NE**	15.2 (T1) 0.396 (T2)
882	MPS II	2.5x10 <sup>12</sup>	1	21	No	Histiocytic sarcoma (liver, spleen)	N/A
151	MPS II	5x10 <sup>12</sup>	1	25	Liver	NE**	2.92
173	MPS II	5x10 <sup>12</sup>	1	16	No	Histiocytic sarcoma (liver, Kidney, spleen)	N/A
206	MPS II	5x10 <sup>12</sup>	1	16	Liver	ND*	1.47
235	MPS II	5x10 <sup>12</sup>	1	25	Liver	ND*	1.42 (T1) 0.785 (T2)
429	MPS II	5x10 <sup>12</sup>	3	17	Liver	ND*	8.220 (T1) 5.07 (T2)
691	MPS II	5x10 <sup>12</sup>	6	22	Liver	ND*	8.60 (T1) 1.00 (T2) 1.23 (T3)
1027	MPS II	1x10 <sup>13</sup>	6	23	Liver	NE**	0.712 (T1) 0.943 (T2)
1035	MPS II	1x10 <sup>13</sup>	6	25	Liver	NE**	1.592
1036	MPS II	1x10 <sup>13</sup>	6	21	Liver	ND*	1.611
1132	MPS II	2x10 <sup>13</sup>	6	21	Liver	ND*	21.9 (T1) 20.7 (T2)
1062	MPS II	2x10 <sup>13</sup>	9	21	Liver	ND*	1.20 (T1) 38.5 (T2)
148	WT	NT	N/A	29	Liver	Histiocytic sarcoma (liver, Kidney, lung)	9 tumors, NE**
294	WT	NT	N/A	28	Liver	ND*	<0.001
677	WT	NT	N/A	24	Liver	ND*	ND*
53	WT	NT	N/A	26	Liver	NE**	<0.001(T1) <0.001(T2)
862	WT	NT	N/A	26	Liver	NE**	<0.001
316	WT	NT	N/A	30	Liver	NE**	<0.001(T1) <0.001(T2) <0.001(T3)
332	WT	NT	N/A	23	Liver	NE**	<0.001
294	WT	NT	N/A	28	Liver	NE**	<0.001
402	WT	NT	N/A	28	Liver	NE**	ND*

<sup>#</sup>: Histopathology examination on H&E-stained non-tumor tissues; \*ND: not detected; \*\*NE: not examined.